

Astro2020 APC White Paper

The CCAT-Prime Submillimeter Observatory

Thematic Areas: ☐ Planetary Systems ☒ Star and Planet Formation
☐ Formation and Evolution of Compact Objects ☒ Cosmology and Fundamental Physics
☒ Stars and Stellar Evolution ☐ Resolved Stellar Populations and their Environments
☒ Galaxy Evolution ☐ Multi-Messenger Astronomy and Astrophysics

Corresponding Author: Terry Herter, Cornell University, tlh10@cornell.edu, 607-257-8432

Co-authors: Nicholas Battaglia (Cornell), Kaustuv Basu (Bonn), Benjamin Beringue (Cambridge), Frank Bertoldi (Bonn), Scott Chapman (Dalhousie), Steve Choi (Cornell), Nicholas Cothard (Cornell), Dongwoo Chung (Stanford), Jens Erler (Bonn), Michel Fich (Waterloo), Simon Foreman (CITA), Patricio Gallardo (Cornell), Jiansong Gao (NIST), Urs Graf (Cologne), Martha Haynes (Cornell), Terry Herter (Cornell), Gene Hilton (NIST), Johannes Hubmayr (NIST), Doug Johnstone (Victoria), Eiichiro Komatsu (MPA), Benjamin Magnelli (Bonn), Phil Maukkopf (ASU), Jeffrey McMahon (Michigan), Daan Meerburg (Cambridge), Joel Meyers (Southern Methodist), Avirukt Mittal (Cornell), Michael Niemack (Cornell), Thomas Nikola (Cornell), Stephen Parshley (Cornell), Dominik Riechers (Cornell), Gordon Stacey (Cornell), Juergen Stutzki (Cologne), Eve Vavagiakis (Cornell), Marco Viero (Stanford), Michael Vissers (NIST)

Executive Summary: The Cerro Chajnantor Atacama Telescope-prime (CCAT-prime) is a new 6-m, off-axis, low-emissivity, large field-of-view submillimeter telescope scheduled for first light in the last quarter of 2021. In summary,

- (a) CCAT-prime uniquely combines a large field-of-view (up to 8-deg), low emissivity telescope ($< 2\%$) and excellent atmospheric transmission (5600-m site) to achieve unprecedented survey capability in the submillimeter.
- (b) Over five years, CCAT-prime *first generation science* will address the physics of star formation, galaxy evolution, and galaxy cluster formation; probe the re-ionization of the Universe; improve constraints on new particle species; and provide for improved removal of dust foregrounds to better constrain primordial inflationary gravity waves.
- (c) The Observatory is being built with non federal funds ($\sim \$40\text{M}$ in private and international investments). Public funding is needed for instrumentation ($\sim \$8\text{M}$) and operations ($\$1\text{-}2\text{M/yr}$). In return, the community will be able to participate in survey planning and gain access to curated data sets.
- (d) For *second generation science*, CCAT-prime will be uniquely positioned to contribute high-frequency capabilities to the next generation of CMB surveys in partnership with the CMB-S4 and/or Simons Observatory projects or revolutionize wide-field, sub-millimeter line intensity mapping surveys.

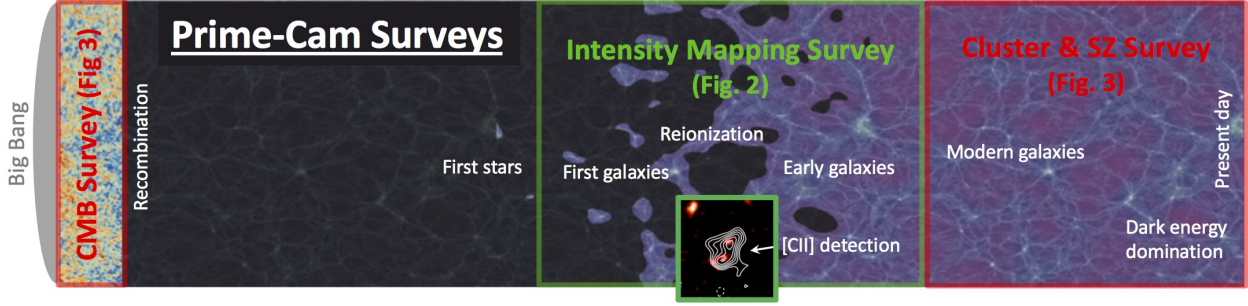


Figure 1: Prime-Cam surveys on a schematic history of the Universe. The three primary science surveys in key legacy survey fields targeted by the planned Prime-Cam observations are: [CII] line intensity mapping of the Epoch of Reionization (EoR, Figure 2), galaxy cluster and Sunyaev-Zeldovich (SZ, Figure 3), and CMB polarization (CMB, Figure 3; image modified from [49]; [CII] detection inset from [48]).

Key Science Goals and Objectives

First generation science:

During its first five years, CCAT-prime will perform a set of wide-area surveys to uniquely address forefront science. Below we give brief descriptions of the different areas. References to relevant Astro2020 White Papers following the science theme titles.

Tracing the epoch of reionization with CII intensity mapping [35, 12, 14, 41]: CCAT-prime will aid in understanding the processes of structure formation and probe the underlying dark matter density fluctuations by mapping the large-scale three-dimensional (3D) clustering of star-forming galaxies. This is done using wide-field spectroscopy of the aggregate [CII] $158\mu\text{m}$ signal from star formation regions in galaxies to perform 3D tomography of the spatial fluctuations due to large-scale structure at $z = 3.5 - 8.0$, all the way from “cosmic noon” into the epoch of reionization [36].

The Prime-Cam instrument [52, 56], described below in the technical overview, will provide maps over several 8 deg^2 survey fields in [CII] emission across this redshift range (Figure 2). It will simultaneously provide measurements of the [OIII] $88\mu\text{m}$ line from HII regions in $z > 7$ galaxies and of multiple CO lines at virtually any redshift. This data will be highly complementary to targeted studies of individual galaxies at the same redshifts with ALMA, ngVLA, JWST, and OST by providing information on the large-scale structure in which those sources are embedded, and the aggregate signal from sources too faint to be individually detected by those facilities.

Understanding galaxies and galaxy cluster formation via millimeter and sub-millimeter observations [5, 39, 7, 43]: CCAT-prime will constrain feedback mechanisms and test cosmological simulations by measuring the thermodynamic properties of galaxies and galaxy clusters via the Sunyaev-Zel’dovich (SZ) effects on the cosmic microwave background (CMB) [42, 6]. CCAT-prime’s 270–350 GHz measurements combined with 30–270 GHz data from Advanced ACTPol (AdvACT) [28] and Simons Observatory (SO) [23] will measure $\sim 16,000$ clusters and detect the fainter kinetic SZ (kSZ) effect to trace the peculiar velocity field in the Universe (the standard thermal SZ effect, tSZ, will be readily detected). The data also allow for

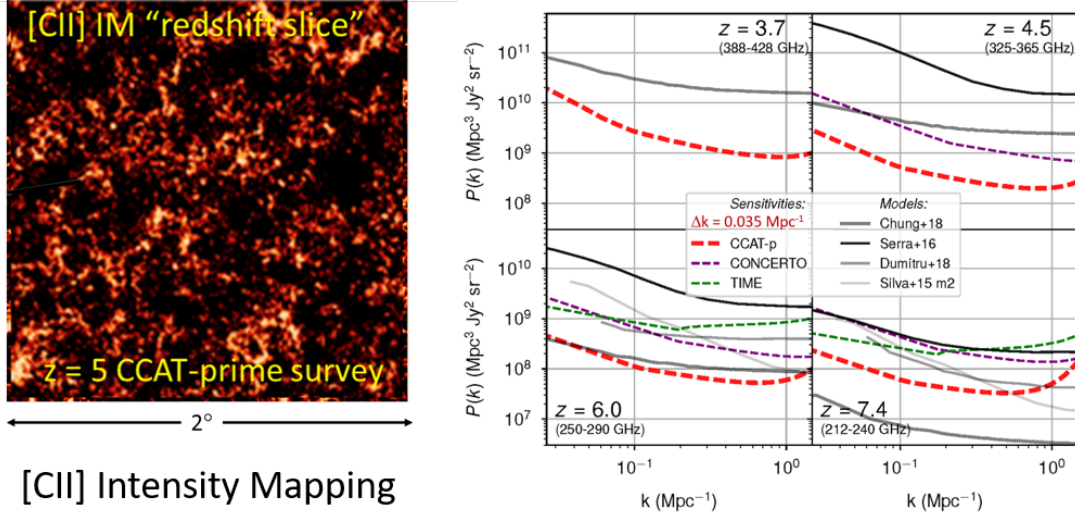


Figure 2: Simulated “redshift slice” (*left*) of the area covered by the [CII] intensity mapping survey in the epoch of reionization (EoR), representing a small spectral bin within the vast $z = 3.5\text{--}8.0$ redshift range covered by the Prime-Cam spectrometer [CII] measurements. *Right*: The power spectrum of the [CII] emission reveals the topology of reionization and the [CII] luminosity fluctuations at redshifts of 3.7 to 7.4 (predictions based on [13]). Recent state-of-the-art model predictions (solid lines) differ by factors of 10 to 50. Overlaid are our predicted EoR-Spec sensitivities for the planned 16 deg^2 first generation survey. Prime-Cam surveys are as much as $10\times$ more sensitive than the other proposed surveys (TIME and CONCERTO; [16, 37]) leading to an expectation for detection of the intensity mapping signal at redshifts approaching 8 for most models. ALMA cannot make these measurements, since its field of view is smaller than a single pixel of EoR-Spec on CCAT-prime, and because it is mainly sensitive to the signal of individual galaxies, rather than the aggregate emission seen by intensity mapping studies.

precise tracing of the SZ spectral shapes of individual clusters enabling measurements of their mean electron temperature (the relativistic SZ effect, rSZ).

With these measurements CCAT-prime will provide valuable complementary information for deriving accurate cluster properties, like masses. Prime-Cam measurements have the potential to enable the detection of all three SZ components (cluster optical depth, bulk velocity, and temperature) and dust emission from individual clusters [22, 42], for a large, statistically significant cluster sample for the first time. Measurements of the tSZ and kSZ effects provide windows into the thermodynamic profiles of individual galaxy clusters and ensemble samples of galaxies, enabling essential tests for feedback mechanisms and for the successful cosmological hydrodynamical simulations that match the optical properties of galaxies in dense environments measured by space and ground-based optical surveys like LSST.

Enhancing constraints on new particle species with Rayleigh Scattering [26]: CCAT-prime will measure Rayleigh scattering of CMB photons for the first time to improve constraints on new particle species, and characterize polarized dust foregrounds that limit constraints on inflation [1, 3]. Prime-Cam’s 270–350 GHz bands open up yet another unexplored window of Rayleigh scattering. Shortly after recombination, CMB photons undergo Rayleigh scattering with neutral

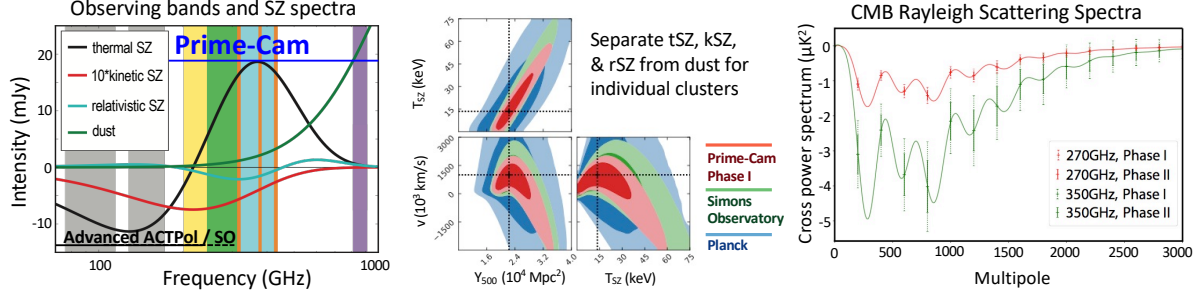


Figure 3: Prime-Cam observations will span from 200 to 900 GHz (*left*), including photometric (green, blue, and purple bands) and spectroscopic observations (yellow through orange bands). Measurements at these frequencies are needed in addition to lower frequency bands (grey and yellow - AdvACT - plus green - SO) to cleanly separate CMB and SZ signals (black, red, blue lines) from dust (green line) that contaminates CMB anisotropies. These observations will enable determination of the temperatures and velocities of galaxy clusters (*middle*, 1σ and 2σ contours shown) [22]. High frequency CMB polarization measurements with Prime-Cam will enable high-S/N measurements of Rayleigh scattering of the CMB for the first time (*right*), which will lead to improvements in cosmological constraints beyond what can be achieved with traditional lower-frequency CMB measurements [3]. Such improvements in cosmological constraints could provide evidence for beyond the standard model particle species and possibly dark matter candidates [8].

hydrogen and helium which produces a strong frequency-dependent cross-section [38]. This has the effect of a frequency-dependent change to the visibility function, suppressing primary CMB temperature fluctuations and generating new polarization at high frequencies and small angular scales, providing access to new modes that probe the early Universe [38] and improvements on cosmological parameters affecting recombination physics [3].

CCAT-prime is uniquely positioned to make the first detection of Rayleigh scattering of the CMB¹ (Fig. 3) and utilize the information from it in future cosmological constraints. The forecasted improvement in cosmological parameters is modest, however, without Rayleigh scattering the constraints on beyond the standard model (BSM) particle species and possibly dark matter candidates requires a factor of > 2 increase in number of detectors or integration time. Thus, CCAT-prime could improve the science return and/or reduce costs by tens of millions of dollars for future, ground-based CMB experiments (CMB-S4 and Simons Observatory) that aim to further constrain these BSM particle species.

Measuring CMB foregrounds to constrain inflation [34]: CCAT-prime will enable more precise constraints on primordial inflationary gravity waves by characterizing dust foregrounds that dilute measurements of CMB polarization [1]. By measuring dust polarization properties above 250 GHz with sub-arcmin resolution and high signal-to-noise ratios using Prime-Cam, we will be able to measure the spectrum and polarization angles of dust emission to inform future surveys and average the results over larger areas to remove dust polarization from low-resolution inflationary gravitational wave experiments [45, 54].

¹It may be possible to detect Rayleigh scattering in the Planck CMB maps. However, it is expected to be at lower significance and CCAT-prime's wide and high resolution frequency coverage will help mitigate foregrounds more effectively [8].

Tracing galaxy evolution from the first billion years to Cosmic Noon with the cosmic infrared background [25]: CCAT-prime will directly trace the evolution of dust-obscured star formation in galaxies since the epoch of galaxy assembly, starting > 10 billion years ago [47, 25]. By combining our CCAT-prime surveys with synergistic work in the optical/near-IR (e.g. LSST, DES, Euclid and WFIRST) we will identify key parameters that regulate star formation (such as environment and matter content) over cosmic time.

Half of the starlight emitted through cosmic time is obscured by dust which absorbs, and re-emits the light that we measure as the cosmic infrared background (CIB)[11, 21]. Therefore, to understand the star formation history of the universe, one must measure it both directly through its optical emission from stars that is redshifted into the near-IR bands, and indirectly from the dust emission redshifted into the submm bands. At redshifts < 1.7 most of the CIB was resolved into individual galaxies by Spitzer and Herschel, yet at earlier times the fraction drops to just 10% [9]. CCAT-prime will probe a factor of 2 to 10 times deeper than the confusion limited Herschel surveys, detecting hundreds of thousands of galaxies to redshifts approaching 7, and unveil about 40% of the star formation at these epochs. The wide-field ($> 400^{\circ 2}$). CCAT-prime surveys sample large-scale environments that cannot be mapped with ALMA, and down to luminosities that are inaccessible to Herschel. CCAT-prime surveys at $350\ \mu\text{m}$ are critical to extracting infrared luminosities and dust-obscured star formation rates at far greater precision than possible with longer wavelength (e.g. $850\ \mu\text{m}$) surveys alone.

The starformation-ISM cycle in local galaxies with high spectral resolution submillimeter observations [10, 51, 53]: CCAT-prime will investigate the life cycle of stars from cloud assembly through the formation of stars and expulsion of material at stellar death feeding back into the next cycle, specifically addressing such questions as: How does galactic environment affect star formation and determines its location (e.g. filaments, galactic arms, nuclear rings), intensity, and efficiency? What is the life-cycle of molecular clouds - the birthplace of stars? Does turbulence trigger, or inhibit star formation?

High spatial resolution over very large fields thereby linking local star formation sites to global parameters are needed to answer these questions. Using the multi-beam heterodyne receiver (CHAI) on CCAT-prime we can reveal structures in the galaxy at size-scales from 0.01 pc to over 4 kpc - a factor of 4×10^5 in scale! CHAI provides the high spectral resolution necessary to trace inflows, outflows and turbulence, and the velocity information necessary to further distinguish among spatially unresolved structures. Surveys will focus on the submillimeter [CI] lines to trace the CO dark molecular gas, and mid-J CO lines to trace the warm, active molecular gas in regions of turbulent dissipation and feedback in the Milky Way and nearby star forming galaxies. The [NII] $205\ \mu\text{m}$ line will be used to trace the ionized gas associated newly formed early-type stars.

A new submillimeter window into time domain astrophysics: CCAT-prime will discover galactic and extragalactic transients at millimeter and submillimeter wavelengths in a survey covering half the sky, including observations of protostar variability (e.g. [61, 30]), gamma-ray burst after glows (e.g. [58]), and potentially new solar system objects (e.g. [15]).

Second generation science:

One of the most compelling research areas in millimeter and submillimeter astrophysics today is using CMB anisotropy measurements to constrain cosmology. The cosmological science enabled by these measurements is well summarized in the CMB-S4 Science Book [1] and several decadal white papers, including [7, 26, 34, 39, 41]. These measurements would also enable great progress in many of the “first generation” science areas described above. The CCAT-prime telescope and site are uniquely capable of advancing the CMB-S4 legacy survey science cases by deploying a second generation “CMB-S4-scale” receiver on CCAT-prime and using it in collaboration with the CMB-S4 and/or Simons Observatory projects to observe the majority of the sky at millimeter and sub-millimeter wavelengths.

The first generation CCAT-prime measurements will contribute to improved characterization of secondary CMB anisotropies, including the SZ effects, gravitational lensing, and Rayleigh scattering. These measurements will inform the second generation CCAT-prime CMB science optimization, which is currently being developed with input from the CMB-S4 and Simons Observatory teams. This collaborative approach has evolved naturally given that the CCAT-prime telescope design was adopted for the Simons Observatory Large Aperture Telescope (SO-LAT) and as the reference design for CMB-S4. As a result, both CMB-S4 and Simons Observatory researchers have at times included submillimeter capabilities being considered for CCAT-prime in science forecasts. For example, CMB-S4 galaxy cluster forecasts clearly demonstrate the added value of CCAT-prime submillimeter measurements for extracting cluster properties [31, 42]. Delensing of primordial gravitational waves from inflation is another area where CCAT-prime provide unique contributions via submillimeter cosmic infrared background (CIB) measurements (e.g. [50, 40]). The complementarity of CIB and CMB delensing will enable valuable cross-checks on both approaches, and depending on the survey areas and complexity of delensing systematics, CIB delensing could potentially prove to be more valuable for constraining inflation.

CCAT-prime is also an ideal platform for wide-field, sub-millimeter line intensity mapping surveys, as its first generation measurements will demonstrate. Improvements in mapping speed by 1-2 orders of magnitude can be achieved by fully populating a next generation cryostat or through switching to spectrometer-on-chip technologies, if they reach maturity in the next 5 years. This would shed light on a wide array of puzzles in galaxy evolution, cosmology, and fundamental physics (e.g.,[35]).

Time-domain measurements, such as searches for additional planets in our solar system [15], measurements of gamma-ray-burst afterglows [58], and stellar variability studies [61] have all been shown to benefit from both the shorter wavelength and improved resolution of CCAT-prime submillimeter bands. The high elevation site and improved surface accuracy of CCAT-prime also provide greater sensitivity for CMB measurements at millimeter wavelengths needed for the core science goals of CMB-S4 and Simons Observatory. This combination of new science capabilities and more sensitive CMB measurements make development of a large camera that utilizes the entire CCAT-prime field of view a high priority this decade.

Technical Overview

The enabling parameters for CCAT-prime are driven by the telescope and site. The 6-m, off-axis, cross-Dragone submillimeter telescope [44] delivers an extraordinarily wide diffraction-limited field-of-view (FoV): from 2° in diameter at 860 GHz (0.35 mm) to 8° at 100 GHz (3 mm). In addition, the observatory will be located at 5600-m on Cerro Chajnantor in the Atacama Desert of Northern Chile above the ALMA Observatory resulting in improved atmospheric transparency [46]. The Observatory will have two first generation instruments, Prime-Cam and CHAI. Prime-Cam will be allocated 75% of the available observing time over the first five years (over 12,000 hours). A second instrument, the CCAT Heterodyne Array Instrument (CHAI) is being constructed by the University of Cologne to perform velocity resolved spectral line observations of the Milky Way and nearby galaxies will use the remaining 25% of the time. Figure 4 shows the nominal performance gain of CCAT-prime relative to other observatories. Continuum survey sensitivity is given in Table 2.

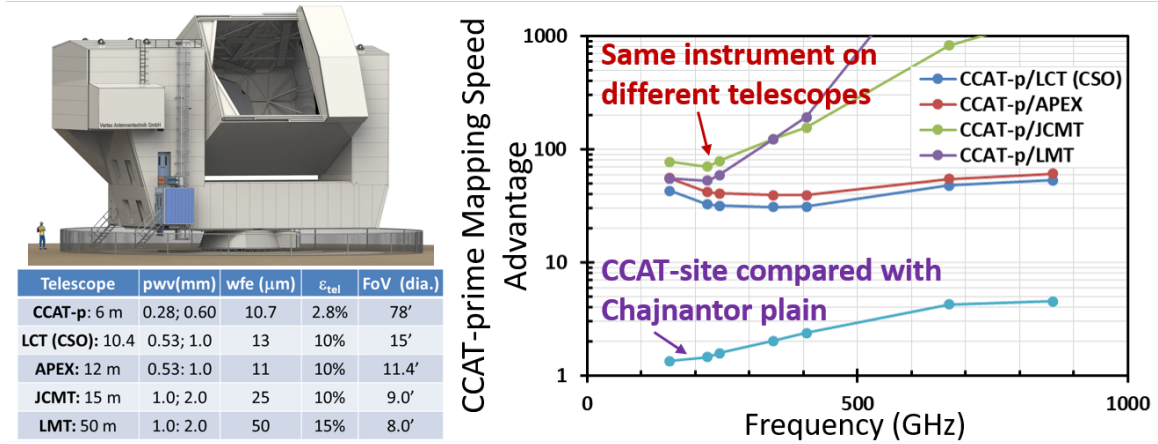


Figure 4: **Site and telescope summary.** *Top Left:* The CCAT-prime telescope is being built by Vertex Antennentechnik. *Right:* Continuum mapping speed comparisons. The top four lines (green [32], purple [59], red [27], and blue [60]) are mapping speed ratios at 45° elevation for a camera with $1.5 \lambda/D$ spaced horns that fills the FoV of a single instrument module in CCAT-prime compared with an identical camera on other coeval telescopes, including the proposed Leighton Chajnantor Telescope (LTC, formerly the CSO) relocation to Chile. We make the comparison for intensity mapping referred to a $1'$ beam for the top two weather quartiles (PWV [46], wave-front error (wfe), emissivity ϵ_{tel} , and field-of-view (FoV) assumptions at left). CCAT-prime is $>20\times$ faster in all cases *per instrument module*. Up to 7 instrument modules like this could be deployed in Prime-Cam. The lower, aqua-colored line shows the mapping speed advantage gain per pixel for the CCAT-site on Cerro Chajnantor over the Chajnantor plain [46]. The similar SO telescope is only designed to observe at <300 GHz (~ 3 left points on curve).

Prime-Cam is a modular instrument capable of supporting up to seven independent instrument modules to pursue complementary science goals ([52], Figure 5). These seven modules, or optics tubes, will support broadband measurements at five different frequencies (220, 270, 350, 410, 860 GHz) in parallel with spectroscopic measurements (with $R = 100$ between 210 – 420 GHz) to enable the science goals described above.

The instrument module design details are presented in several recent conference proceedings,

including [56, 19, 62, 24]. The nominal module design is being developed collaboratively with the Simons Observatory, but critical changes to the module designs are needed to achieve the CCAT-prime science goals. Each broadband polarization-sensitive module will include filters, lenses, and three 15 cm diameter detector arrays. The CCAT-prime spectrometer modules require low-temperature Fabry-Perot Interferometer optics that will be installed at the Lyot stop in the relevant modules. For millimeter wavelength detectors the most mature and compelling detector technology is superconducting transition-edge-sensor (TES) bolometers read out by SQUIDs [57, 17]. However, it appears that readout challenges will limit development of TES arrays with more than ~ 2000 detectors per 15 cm array (e.g., [2]), which is significantly fewer than the optimal number of detectors at submillimeter wavelengths (and even up to ~ 1.4 mm) on CCAT-prime. The most promising detector technology for these submillimeter wavelengths is kinetic inductance detectors, which offer the potential for greatly simplified readout (see below) [18, 33].

The second generation CCAT-prime instrument follows the CMB-S4 reference design, which is similar to Prime-Cam but includes nineteen instrument modules instead of only seven (Figure 5). This combined with the deployment of more detector arrays per module (as described in the CMB-S4 decadal survey report) will boost the mapping speed of CCAT-prime by roughly a factor of four compared to a fully populated Prime-Cam.

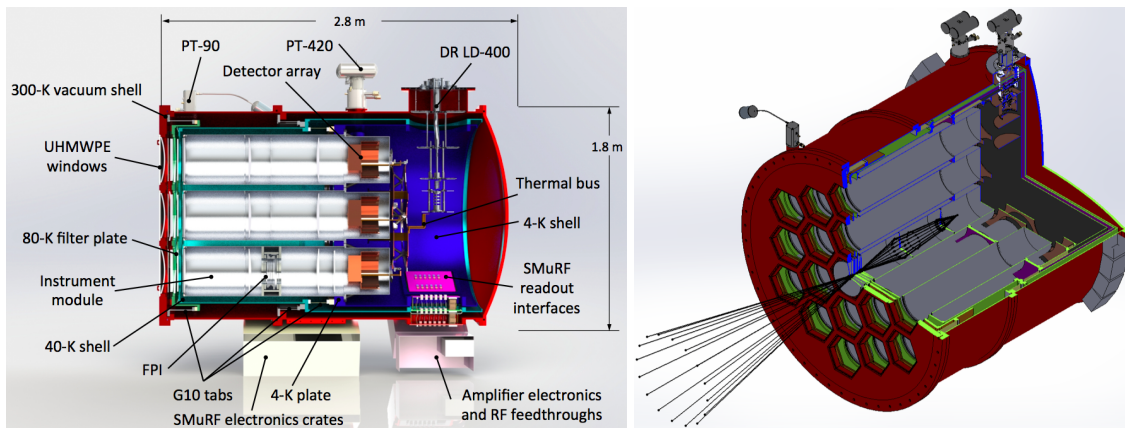


Figure 5: *Left:* Cutaway of the Prime-Cam cryostat, which is capable of housing seven instrument modules [56]. *Right:* Preliminary design for the second generation nineteen module CCAT-prime instrument. Note that this cryostat is considerably larger than Prime-Cam, while the instrument modules inside both cryostats are the same size. This model was developed in parallel with the Simons Observatory thirteen module cryostat [62] and has recently been adopted as the CMB-S4 reference design.

Technology Drivers:

Several of the technology drivers for the measurements described above are being addressed and optimized by a combination of efforts from CCAT-prime, SO, and CMB-S4.

Both CCAT-prime and Simons Observatory are building and will soon be deploying instrument modules (also known as optics tubes) that will serve as prototypes for a project at the CMB-S4

scale. When observations begin, these modules will be the largest scale deployment of superconducting TES detectors yet. The CMB-S4 project is also supporting research and development that is important for scaling these projects to CMB-S4 sensitivity, systematics, and instrument production levels.

As described above, current TES detector array technologies that can read out two kilopixels per detector wafer [29, 2] are well matched to the CCAT/SO instrument module designs for wavelengths longer than ~ 1.4 mm. At shorter submillimeter wavelengths the sensitivity can be improved considerably by increasing the number of detectors per wafer. The most promising approach for this in the coming decade is using KIDs instead of TESes due to the much simpler readout architecture. KIDs are being used successfully for astrophysical measurements in the NIKA-2 instrument on IRAM [55], and will soon be deployed on both the BLAST-TNG balloon observatory [20] and the Toltec camera for the LMT [4]. However, none of those projects will reach the required readout scale to take full advantage of Prime-Cam on CCAT-prime.

Breakthroughs in submillimeter astrophysics in the coming decade will require advances in submillimeter detector arrays and readout. Prime-Cam on CCAT-prime is the ideal platform to enable these advances by deploying submillimeter detector arrays with $\sim 10^5$ detectors and using them for novel measurements. KID detector arrays are rapidly exceeding the detector densities of TES arrays, such as the Toltec 270 GHz array with over 4000 KIDs per wafer, compared to 2000 TESes on the highest density wafers. For CCAT-prime at first light we plan to deploy KID arrays operating at both 270 GHz and 350 GHz that will each have over 4000 KIDs. Scaling the 270 GHz array to 860 GHz with the same $F\lambda$ pixel spacing would result in over 40,000 KIDs per wafer. A fully populated Prime-Cam instrument could illuminate 3 wafers at 860 GHz and 18 wafers at 270 and 350 GHz, which sums to roughly 200,000 detectors!

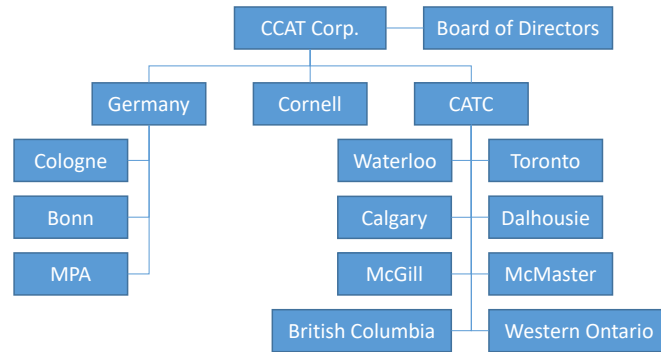
Deploying detector arrays at this scale is a high priority for submillimeter astrophysics, although, the readout technologies required for this need additional development. Fortunately, industry is driving advances in microwave systems, and the new Xilinx software defined radio RFSoc system² includes the hardware to meet the needs of next generation KID readout. Specifically, each RFSoc has sufficient bandwidth to acquire data from roughly 5000 KIDs, which is almost ten times more than existing KID readout systems (such as the ROACH-2). In other words, approximately 40 Xilinx RFSoc boards would be needed to readout a fully populated Prime-Cam, versus, approximately 400 ROACH-2 systems. The RFSocs are not yet ready for use due to the need to develop KID optimized RFSoc firmware, which can then be tested and deployed on astronomical observatories like CCAT-prime. In addition to submillimeter astrophysics, this readout development research is expected to benefit observatories operating at many other wavelengths spanning from optical to radio. CCAT-prime is an ideal telescope for the initial deployment of these technologies because of the high-throughput, modularity, relatively low operating costs, and flexibility of the team.

The combination of the ongoing instrument module development combined with support for development of submillimeter KID arrays and readout systems for Prime-Cam will enable the technology advances needed for both CMB-S4-scale instruments and next generation submillimeter astrophysics.

²Xilinx RFSoc website: <https://www.xilinx.com/products/silicon-devices/soc/rfsoc.html>

Organization, Partnerships, and Current Status: CCAT-prime is being built by CCAT Corporation which is independently funded by an international consortium consisting of Cornell University, a German partnership led by the University of Cologne, and a Canadian partnership led by the University of Waterloo. Figure 6 shows organizational chart and member institutions. The Tokyo Atacama Observatory (TAO) shares the mountain top. CCAT has a draft agreement to share common costs such as road maintenance, power, etc. With funding from NSF (or other public sources), CCAT-prime will bring in community members to participate in survey planning and provide general access to curated data sets.

Figure 6: CCAT organization chart showing members of the German and Canadian (CATC) consortia. Other participants in Canada include St. Mary's University, University of Manitoba, University of Lethbridge and University of Alberta. The Board of Directors has representatives from the these two consortia and Cornell.



Schedule: The telescope is being built by Vertex Antennentechnik GmbH under a fixed-price contract to the CCAT corporation. An in situ laser interferometric metrology system developed by Etalon-AG (Germany) will be used to align the mirror panels to a few microns. Site preparation and development (civil works) are performed in parallel with the telescope construction. Figure 7 shows the schedule. Fabrication of long lead items for the telescope is underway. To ensure efficient and safe assembly on the mountain, the telescope is fully assembled and aligned in Europe, and then partly disassembled for shipment to Chile. Following re-assembly on the mountain, the surface accuracy will be verified using the laser system and tower holography.

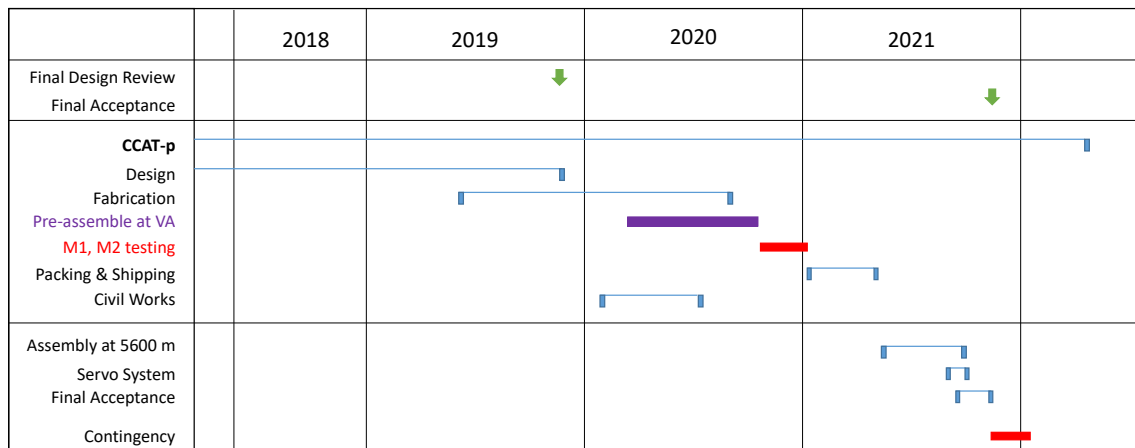


Figure 7: Top-level CCAT-prime observatory schedule showing major milestones. First light is scheduled for the last quarter of 2021. The initial science surveys occupy the first five years of operations. The observatory would then nominally transition to second generation science. The lifetime of the observatory is expected to be 10-20 years.

Cost Estimates: Table 1 gives the run out costs in real year dollars for CCAT-prime. These estimates are updated quarterly. The basis of costs for the Observatory are a fixed-price contract for the telescope and bids for the infrastructure work. The facility operations costs are based on a bottoms-up estimate (fuel, road maintenance, site fees, on-going maintenance, etc.). Science operations are based on sizing of the team to handle data reduction and analysis, curation and maintenance of the archive for the community, support of workshops for the community, etc.).

Also included in Table 1 are funding commitments from private and international sources and aspirational funding from federal sources. Although the construction of CCAT-prime is covered by private and international funding, public funding is needed to complete the Prime-Cam instrument and support operations. The total funding line includes five years of operations.

CCAT-prime is ideally suited to participate in the next generation of CMB Stage-4 scale science for which the costs will be of order \$30 - 50M for instrumentation and operations.

Table 1: Costs and Contributions

Item	Cost (M\$)	Contribution			Comments
		Federal ^a (M\$)	International (M\$)	Private (M\$)	
Observatory	26.5 ^b	-	10	17.35	includes telescope and infrastructure
Prime-Cam ^c	13	8	2	3	first-light instrument
CHAI ^d	9	-	9	-	first-light instrument
Facility Ops/yr	2.5	1	1	0.5	
Science Ops/yr	2	1	1	-	
Total	71.5	18	31	22.85	through 5 years of operations

^a Aspirational funding levels for instrument development and operations. ^b Excludes cost of constructing power plant on plateau. ^c Prime-Cam can support up to 7 science modules at a cost of approximately \$2M per modules based on currently technologies. The baseline is 2 modules at first-light with 3 more added within 2 years. ^d Fully funded by German consortium.

Table 2: Overview of baseline Prime-Cam survey performance [52]

Survey	Field ID	LST range [h]	Area [deg ²]	Time [hr]	Sensitivity ^c (@ representative ν_{obs} [GHz])	Supporting Surveys ^b
EoR ^a	E-COSMOS	7.0-13.0	8	2000	0.02 MJy sr ⁻¹ bin ⁻¹ @ 220	1
	E-CDFS	23.5-7.0	8	2000	0.02 MJy sr ⁻¹ bin ⁻¹ @ 220	2
	HERA-Dark	13.0-23.5	8	(filler)	0.02 MJy sr ⁻¹ bin ⁻¹ @ 220	3
DSFG	Stripe 82	20.0-5.5	300	500	2.5 mJy beam ⁻¹ @ 860	4
	GAMA9/12/15	5.5-20.0	110	180	2.5 mJy beam ⁻¹ @ 860	5
SZ/CMB	AdvACT/SO	all	12,000	4000	11 μ K/arcmin ² (CMB) @ 270	6

^aSpectroscopy; sensitivities provided for $R=100$. ^b(1) Deep Subaru HSC+PSF spectroscopy & COSMOS X-Ray-to-meter-wave multiwavelength survey; (2) deep Euclid grism spectroscopy (upcoming), HERA HI 21 cm (upcoming), & H-UDF/CDF-S multiwavelength surveys (incl. JWST GTO); (3) HERA HI 21 cm (upcoming), VLASS; (4) SDSS, HeLMS/HeRS Herschel/SPIRE, VLASS; (5) GAMA, H-ATLAS Herschel/SPIRE, ACT, VLASS; (6) Planck, SDSS, DES, ACT, SO, DESI, LSST, eROSITA (upcoming).

^cPreliminary model; an enhanced noise model will be presented by Choi, S. et al. (2019), in prep.

References

- [1] K. N. Abazajian, P. Adshead, Z. Ahmed, et al., 2016, CMB-S4 Science Book, First Edition, *ArXiv e-prints*, [ArXiv](#).
- [2] M. H. Abitbol, Z. Ahmed, D. Barron, et al., 2017, CMB-S4 Technology Book, First Edition, *ArXiv e-prints*, [ArXiv](#).
- [3] E. Alipour, K. Sigurdson, and C. M. Hirata, 2015, Effects of Rayleigh scattering on the CMB and cosmic structure, *Phys. Rev.*, D91(8), 083520, [Pub](#), [ArXiv](#).
- [4] J. E. Austermann, J. A. Beall, S. A. Bryan, et al., 2018, Millimeter-Wave Polarimeters Using Kinetic Inductance Detectors for TolTEC and Beyond, *ArXiv e-prints*, [ArXiv](#).
- [5] K. Basu, J. Erler, J. Chluba, et al., 2019, “SZ spectroscopy” in the coming decade: Galaxy cluster cosmology and astrophysics in the submillimeter, in *BAAS*, vol. 51, 302, [ArXiv](#).
- [6] N. Battaglia, S. Ferraro, E. Schaan, et al., 2017, Future constraints on halo thermodynamics from combined Sunyaev-Zel’dovich measurements, *ArXiv e-prints*, [ArXiv](#).
- [7] N. Battaglia, J. C. Hill, S. Amodeo, et al., 2019, Probing Feedback in Galaxy Formation with Millimeter-wave Observations, in *BAAS*, vol. 51, 297, [ArXiv](#).
- [8] B. Beringue, P. D. Meerburg, and J. Meyers, 2018, Cosmology with Rayleigh Scattering, *in prep*.
- [9] M. Béthermin, E. Le Floc’h, O. Ilbert, et al., 2012, HerMES: deep number counts at 250 μm , 350 μm and 500 μm in the COSMOS and GOODS-N fields and the build-up of the cosmic infrared background, *Ast. and Ap.*, 542, A58, [Pub](#), [ArXiv](#).
- [10] A. Bolatto, L. Armus, S. Veilleux, et al., 2019, Cold Gas Outflows, Feedback, and the Shaping of Galaxies, in *Bulletin of the American Astronomical Society*, vol. 51 of *BAAS*, 71.
- [11] D. Burgarella, V. Buat, C. Gruppioni, et al., 2013, Herschel PEP/HerMES: the redshift evolution ($0 \leq z \leq 4$) of dust attenuation and of the total (UV+IR) star formation rate density, *Ast. and Ap.*, 554, A70, [Pub](#), [ArXiv](#).
- [12] T.-C. Chang, A. Beane, O. Dore, et al., 2019, Tomography of the Cosmic Dawn and Reionization Eras with Multiple Tracers, in *Bulletin of the American Astronomical Society*, vol. 51 of *BAAS*, 282, [ArXiv](#).
- [13] D. T. Chung, M. P. Viero, S. E. Church, et al., 2018, Forecasting [C II] line-intensity mapping measurements between the end of reionization and the epoch of galaxy assembly, *arXiv e-prints*, arXiv:1812.08135, [ArXiv](#).
- [14] A. Cooray, J. Aguirre, Y. Ali-Haïmoud, et al., 2019, Cosmic Dawn and Reionization: Astrophysics in the Final Frontier, in *Bulletin of the American Astronomical Society*, vol. 51 of *BAAS*, 48, [ArXiv](#).

- [15] N. B. Cowan, G. Holder, and N. A. Kaib, 2016, Cosmologists in Search of Planet Nine: The Case for CMB Experiments, *Ap. J. Lett.*, 822(1), L2, [Pub](#), [ArXiv](#).
- [16] A. T. Crites, J. J. Bock, C. M. Bradford, et al., 2014, The TIME-Pilot intensity mapping experiment, vol. 9153 of *Proc. SPIE*, 91531W, [Pub](#).
- [17] K. T. Crowley, S. M. Simon, M. Silva-Feaver, et al., 2018, Studies of systematic uncertainties for Simons Observatory: detector array effects, in *Proc. SPIE*, vol. 10708 of *Society of Photo-Optical Instrumentation Engineers (SPIE) Conference Series*, 107083Z, [Pub](#), [ArXiv](#).
- [18] P. K. Day, H. G. LeDuc, B. A. Mazin, et al., 2003, A broadband superconducting detector suitable for use in large arrays, *Nature*, 425, 817, [Pub](#).
- [19] S. R. Dicker, P. A. Gallardo, J. E. Gudmundsson, et al., 2018, Cold optical design for the large aperture Simons' Observatory telescope, in *Proc. SPIE*, vol. 10700 of *Society of Photo-Optical Instrumentation Engineers (SPIE) Conference Series*, 107003E, [Pub](#), [ArXiv](#).
- [20] B. Dober, J. A. Austermann, J. A. Beall, et al., 2016, Optical Demonstration of THz, Dual-Polarization Sensitive Microwave Kinetic Inductance Detectors, *Journal of Low Temperature Physics*, 184, 173, [Pub](#), [ArXiv](#).
- [21] H. Dole, G. Lagache, J.-L. Puget, et al., 2006, The cosmic infrared background resolved by Spitzer. Contributions of mid-infrared galaxies to the far-infrared background, *Ast. and Ap.*, 451, 417, [Pub](#), [ArXiv](#).
- [22] J. Erler, K. Basu, J. Chluba, et al., 2018, Planck's view on the spectrum of the Sunyaev-Zeldovich effect, *MNRAS*, 476, 3360, [Pub](#), [ArXiv](#).
- [23] N. Galitzki, A. Ali, K. S. Arnold, et al., 2018, The Simons Observatory: instrument overview, in *Proc. SPIE*, vol. 10708 of *Proc. SPIE*, 1070804, [Pub](#), [ArXiv](#).
- [24] P. A. Gallardo, J. Gudmundsson, B. J. Koopman, et al., 2018, Systematic uncertainties in the Simons Observatory: optical effects and sensitivity considerations, in *Proc. SPIE*, vol. 10708 of *Society of Photo-Optical Instrumentation Engineers (SPIE) Conference Series*, 107083Y, [Pub](#), [ArXiv](#).
- [25] J. Geach, M. Banerji, F. Bertoldi, et al., 2019, The case for a 'sub-millimeter SDSS': a 3D map of galaxy evolution to z 10, in *Bulletin of the American Astronomical Society*, vol. 51 of *BAAS*, 549, [ArXiv](#).
- [26] D. Green, M. A. Amin, J. Meyers, et al., 2019, Messengers from the Early Universe: Cosmic Neutrinos and Other Light Relics, in *BAAS*, vol. 51, 159, [ArXiv](#).
- [27] R. Güsten, L. Å. Nyman, P. Schilke, et al., 2006, The Atacama Pathfinder EXperiment (APEX) - a new submillimeter facility for southern skies -, *Ast. and Ap.*, 454, L13, [Pub](#).
- [28] S. W. Henderson, R. Allison, J. Austermann, et al., 2016, Advanced ACTPol Cryogenic Detector Arrays and Readout, *Journal of Low Temperature Physics*, 184(3-4), 772, [Pub](#), [ArXiv](#).

- [29] S. W. Henderson, J. R. Stevens, M. Amiri, et al., 2016, Readout of two-kilopixel transition-edge sensor arrays for Advanced ACTPol, vol. 9914 of *Proc. SPIE*, 99141G, [Pub](#), [ArXiv](#).
- [30] G. J. Herczeg, D. Johnstone, S. Mairs, et al., 2017, How Do Stars Gain Their Mass? A JCMT/SCUBA-2 Transient Survey of Protostars in Nearby Star-forming Regions, *Ap. J.*, 849, 43, [Pub](#), [ArXiv](#).
- [31] C. Hill, 2019, Communication regarding CMB-S4 LAT Frequency Flowdown.
- [32] W. S. Holland, E. I. Robson, W. K. Gear, et al., 1999, SCUBA: a common-user submillimetre camera operating on the James Clerk Maxwell Telescope, *MNRAS*, 303, 659, [Pub](#), [ArXiv](#).
- [33] J. Hubmayr, J. Beall, D. Becker, et al., 2015, Photon-noise limited sensitivity in titanium nitride kinetic inductance detectors, *Applied Physics Letters*, 106(7), 073505, [Pub](#), [ArXiv](#).
- [34] R. Kallosh and A. Linde, 2019, B-mode Targets, *arXiv e-prints*, arXiv:1906.04729, [ArXiv](#).
- [35] E. Kovetz, P. C. Breysse, A. Lidz, et al., 2019, Astrophysics and Cosmology with Line-Intensity Mapping, in *Bulletin of the American Astronomical Society*, vol. 51 of *BAAS*, 101, [ArXiv](#).
- [36] E. D. Kovetz, M. P. Viero, A. Lidz, et al., 2017, Line-Intensity Mapping: 2017 Status Report, *ArXiv e-prints*, [ArXiv](#).
- [37] G. Lagache, 2018, Exploring the dusty star-formation in the early Universe using intensity mapping, in V. Jelić and T. van der Hulst, eds., *Peering towards Cosmic Dawn*, vol. 333 of *IAU Symposium*, 228–233, [Pub](#), [ArXiv](#).
- [38] A. Lewis, 2013, Rayleigh scattering: blue sky thinking for future CMB observations, *JCAP*, 1308, 053, [Pub](#), [ArXiv](#).
- [39] A. Mantz, S. W. Allen, N. Battaglia, et al., 2019, The Future Landscape of High-Redshift Galaxy Cluster Science, in *BAAS*, vol. 51, 279, [ArXiv](#).
- [40] A. Manzotti, K. T. Story, W. L. K. Wu, et al., 2017, CMB Polarization B-mode Delensing with SPTpol and Herschel, *Ap. J.*, 846(1), 45, [Pub](#), [ArXiv](#).
- [41] P. D. Meerburg, D. Green, M. Abidi, et al., 2019, Primordial Non-Gaussianity, *arXiv e-prints*, arXiv:1903.04409, [ArXiv](#).
- [42] A. Mittal, F. de Bernardis, and M. D. Niemack, 2018, Optimizing measurements of cluster velocities and temperatures for CCAT-prime and future surveys, *JCAP*, 2018(2), 032, [Pub](#), [ArXiv](#).
- [43] T. Mroczkowski, D. Nagai, P. Andreani, et al., 2019, A High-resolution SZ View of the Warm-Hot Universe, in *Bulletin of the American Astronomical Society*, vol. 51 of *BAAS*, 124, [ArXiv](#).

- [44] M. D. Niemack, 2016, Designs for a large-aperture telescope to map the CMB 10x faster, *Applied Optics*, 55, 1686, [Pub](#), [ArXiv](#).
- [45] J. Poh and S. Dodelson, 2017, Line-of-sight extrapolation noise in dust polarization, *Phys. Rev. D*, 95(10), 103511, [Pub](#), [ArXiv](#).
- [46] S. J. E. Radford and J. B. Peterson, 2016, Submillimeter Atmospheric Transparency at Mauna Kea, at the South Pole, and at Chajnantor, *PASP*, 128(7), 075001, [Pub](#), [ArXiv](#).
- [47] D. A. Riechers, 2013, Astronomy: New distance record for galaxies, *Nature*, 502, 459, [Pub](#).
- [48] D. A. Riechers, C. L. Carilli, P. L. Capak, et al., 2014, ALMA Imaging of Gas and Dust in a Galaxy Protocluster at Redshift 5.3: [C II] Emission in “Typical” Galaxies and Dusty Starbursts ~ 1 Billion Years after the Big Bang, *Ap. J.*, 796, 84, [Pub](#), [ArXiv](#).
- [49] B. E. Robertson, R. S. Ellis, J. S. Dunlop, et al., 2010, Early star-forming galaxies and the reionization of the Universe, *Nature*, 468, 49, [Pub](#), [ArXiv](#).
- [50] B. D. Sherwin and M. Schmittfull, 2015, Delensing the CMB with the cosmic infrared background, *Phys. Rev. D*, 92(4), 043005, [Pub](#), [ArXiv](#).
- [51] R. Simon, N. Schneider, F. Bigiel, et al., 2019, The Cycling of Matter from the Interstellar Medium to Stars and back, in *Bulletin of the American Astronomical Society*, vol. 51 of *BAAS*, 367, [ArXiv](#).
- [52] G. J. Stacey, M. Aravena, K. Basu, et al., 2018, CCAT-Prime: science with an ultra-widefield submillimeter observatory on Cerro Chajnantor, in *Proc. SPIE*, vol. 10700 of *Society of Photo-Optical Instrumentation Engineers (SPIE) Conference Series*, 107001M, [Pub](#), [ArXiv](#).
- [53] T. Stanke, H. Beuther, J. Kauffmann, et al., 2019, The warm and dense Galaxy - tracing the formation of dense cloud structures out to the Galactic Center, in *Bulletin of the American Astronomical Society*, vol. 51 of *BAAS*, 542, [ArXiv](#).
- [54] K. Tassis and V. Pavlidou, 2015, Searching for inflationary B modes: can dust emission properties be extrapolated from 350 GHz to 150 GHz?, *MNRAS*, 451, L90, [Pub](#), [ArXiv](#).
- [55] J. van Rantwijk, M. Grim, D. van Loon, et al., 2016, Multiplexed Readout for 1000-Pixel Arrays of Microwave Kinetic Inductance Detectors, *IEEE Transactions on Microwave Theory Techniques*, 64, 1876, [Pub](#), [ArXiv](#).
- [56] E. M. Vavagiakis, Z. Ahmed, A. Ali, et al., 2018, Prime-Cam: a first-light instrument for the CCAT-prime telescope, vol. 10708 of *Proc. SPIE*, 107081U, [Pub](#), [ArXiv](#).
- [57] E. M. Vavagiakis, S. W. Henderson, K. Zheng, et al., 2017, Magnetic Sensitivity of AlMn TESes and Shielding Considerations for Next Generation CMB Surveys, *ArXiv e-prints*, [ArXiv](#).
- [58] N. Whitehorn, T. Natoli, P. A. R. Ade, et al., 2016, Millimeter Transient Point Sources in the SPTpol 100 Square Degree Survey, *Ap. J.*, 830(2), 143, [Pub](#), [ArXiv](#).

- [59] G. W. Wilson, J. E. Austermann, T. A. Perera, et al., 2008, The AzTEC mm-wavelength camera, *MNRAS*, 386, 807, [Pub](#), [ArXiv](#).
- [60] D. Woody, D. Vail, and W. Schaal, 1994, Design, construction, and performance of the Leighton 10.4-m-diameter radio telescopes., *IEEE Proceedings*, 82, 673.
- [61] H. Yoo, J.-E. Lee, S. Mairs, et al., 2017, The JCMT Transient Survey: Detection of Submillimeter Variability in a Class I Protostar EC 53 in Serpens Main, *Ap. J.*, 849, 69, [Pub](#), [ArXiv](#).
- [62] N. Zhu, J. L. Orlowski-Scherer, Z. Xu, et al., 2018, Simons Observatory large aperture telescope receiver design overview, in *Proc. SPIE*, vol. 10708 of *Society of Photo-Optical Instrumentation Engineers (SPIE) Conference Series*, 1070829, [Pub](#), [ArXiv](#).